



# Tracing the second stage of ozone recovery in the Antarctic ozone-hole with a “big data” approach to multivariate regressions

A. T. J. de Laat, R. J. van der A, and M. van Weele

Royal Netherlands Meteorological Institute, De Bilt, the Netherlands

Correspondence to: A. T. J. de Laat (laatdej@knmi.nl)

Received: 28 May 2014 – Published in Atmos. Chem. Phys. Discuss.: 14 July 2014

Revised: 20 November 2014 – Accepted: 25 November 2014 – Published: 8 January 2015

**Abstract.** This study presents a sensitivity analysis of multivariate regressions of recent springtime Antarctic vortex ozone trends using a “big data” ensemble approach.

Our results indicate that the poleward heat flux (Eliassen–Palm flux) and the effective chlorine loading respectively explain most of the short-term and long-term variability in different Antarctic springtime total ozone records. The inclusion in the regression of stratospheric volcanic aerosols, solar variability and the quasi-biennial oscillation is shown to increase rather than decrease the overall uncertainty in the attribution of Antarctic springtime ozone because of large uncertainties in their respective records.

Calculating the trend significance for the ozone record from the late 1990s onwards solely based on the fit of the effective chlorine loading is not recommended, as this does not take fit residuals into account, resulting in too narrow uncertainty intervals, while the fixed temporal change of the effective chlorine loading does not allow for any flexibility in the trends.

When taking fit residuals into account in a piecewise linear trend fit, we find that approximately 30–60% of the regressions in the full ensemble result in a statistically significant positive springtime ozone trend over Antarctica from the late 1990s onwards. Analysis of choices and uncertainties in time series show that, depending on choices in time series and parameters, the fraction of statistically significant trends in parts of the ensemble can range from negligible to a complete 100% significance. We also find that, consistent with expectations, the number of statistically significant trends increases with increasing record length.

Although our results indicate that the use multivariate regressions is a valid approach for assessing the state of Antarctic ozone hole recovery, and it can be expected that

results will move towards more confidence in recovery with increasing record length, uncertainties in choices currently do not yet support formal identification of recovery of the Antarctic ozone hole.

## 1 Introduction

An important question in 21st century ozone research is whether the ozone layer is starting to recover as a result of the measures taken to reduce emissions of ozone-depleting substances (ODSs) as agreed on in the Montreal Protocol (UNEP, 2012) and its subsequent amendments and adjustments.

The World Meteorological Organization has defined three different stages of ozone recovery (WMO, 2007). The first stage consists of a slowing of ozone depletion, identified as the occurrence of a statistically significant reduction in the rate of decline in ozone due to changing stratospheric halogens. The second stage revolves around the onset of ozone increase (turnaround), identified as *the occurrence of statistically significant increases in ozone – above a previous minimum value – that can be attributed to declining stratospheric halogens*. Note that what is meant by “statistically significant” is not specified. Finally, the third stage is the full recovery of ozone from ODSs, identified as when the ozone layer is no longer affected by ODSs, or alternatively, once stratospheric ozone levels have returned to pre-1980 values.

The first stage of ozone recovery has already been identified in observations to have occurred roughly in the late 1990s (WMO 2007, 2011). The third stage is not expected to occur until somewhere halfway through the 21st century or later (WMO, 2011). The spatial distribution of total ozone

after the third stage probably differs somewhat from the pre-1980 distribution due to climate change – in particular changes in the stratospheric chemical composition and temperature structure (Bekki et al., 2011, and references therein).

As far as the second stage of ozone recovery is concerned, it has recently been argued that a statistically significant increase in ozone – beyond a minimum – that is attributable to decreases in ODSs can be identified for the Antarctic ozone hole (Salby et al., 2011, 2012; Kuttippurath et al., 2013; Knibbe et al., 2014). To some extent this is surprising as it has long been thought that identification of the second stage of ozone recovery could only be expected after 2020 (e.g., Newman et al., 2006; Eyring et al., 2007). Those estimates were based on (model) simulations of ozone from which it is calculated when the ozone trend from a certain starting year onwards would qualify for “statistically significant”, or, in other words, would emerge from the year-to-year natural variations in ozone (“noise”). Such methods implicitly assume that ozone variations around the trend are not deterministic (random).

However, it has also long been established that many stratospheric ozone variations are in fact deterministic. Various processes have been identified that affect stratospheric ozone variability in the Southern Hemisphere on an inter-annual basis, like volcanic aerosols (Telford et al., 2009), the Southern Annular Mode (SAM) (Thompson and Wallace, 2000; Jiang et al., 2008), the poleward heat flux or Eliassen–Palm flux (EP flux) (Randel et al., 2002), solar variability (Soukharev and Hood, 2006), and the quasi-biennial oscillation (QBO) (Jiang et al., 2008). If the physics and chemistry are sufficiently understood, it might be possible to filter out part of the ozone variations from the ozone records by means of a multivariate regression, resulting in a smoother ozone record for which trend significance might be reached earlier. This approach, in essence, forms the basis of the suggested identification of the second stage of ozone recovery reported by Salby et al. (2011, 2012), Kuttippurath et al. (2013) and Knibbe et al. (2014).

However, none of these studies systematically considered the uncertainties in the proxies that were selected for the regressions. In addition, no motivation or discussion was provided for the choice of a specific ozone record, e.g., a consideration of taking annual, seasonal and/or monthly means of total ozone, and the integration over a chosen spatial domain.

Hence, we want to address the following question in this study: is the suggested detection of the second stage of ozone recovery robust when uncertainties in the regression parameters and for different selected ozone records are taken into account? This question is approached here with combined multiple-scenario – Monte Carlo ensemble simulations using the same regression methodology as presented in Kuttippurath et al. (2013) but by inclusion of various uncertainties leading to a large ensemble of different regressions. We analyze this “big data” ensemble for robustness of the individual regressions.

Kuttippurath et al. (2013) considered different Antarctic vortex definitions and thus different vortex ozone records. They found that regression results were not very sensitive to the Antarctic vortex definition. Hence, we decided to use September–November Antarctic vortex core (poleward of 70° S) average total ozone column based on the Multi Sensor Reanalysis (MSR; van der A et al. 2010), also because, from a practical point of view, this definition does not require additional information about the location of the vortex edge. The selected regressors are the SAM, solar flux, QBO, EP flux, stratospheric volcanic aerosols and the equivalent effective stratospheric chlorine (EESC), similar to Kuttippurath et al. (2013). The EESC can be used to estimate ozone trends. Kuttippurath et al. (2013) also calculated piecewise linear trends (PWL) for estimating ozone trends as alternative for the EESC-based ozone trends, an approach we will follow here as well.

In this paper, we extend the analysis by introducing both several differing scenarios for the ozone record and regressor records of the EP flux, volcanic aerosols and EESC. Monte Carlo variations were applied to the regressor records of the solar flux, QBO and SAM by adding random variations. While we focus on parameter uncertainties in this study, additional uncertainties do exist, for example with respect to possible time lags between regressors and the ozone record. The resulting ensemble of regression results provides a big data pool of about 23 million different regressions that is analyzed in terms of probability distributions of the explanatory power of the regressions ( $R^2$ ), the ozone trends and corresponding ozone trend uncertainties, and the regression coefficient values quantifying the dependence of ozone on a particular regressor. We also investigate whether some way of optimization is possible for the chosen scenarios, and we discuss the likelihood of detection of the second stage of ozone recovery within the context of all uncertainties presented. Note that the uncertainties discussed here differ from formal errors that come with a standard multivariate regression. Also note that we implicitly assume that the relation between the independent variables and ozone is linear, even though the relation may very well be nonlinear. The latter will to some extent be considered in our study and is part of the discussion of the results, but the issue of nonlinearity of the regressor–ozone relation is not addressed in detail, in particular because, as will be shown, for many regressors the nonlinearity of its relation with ozone is insufficiently characterized, or even unknown.

This paper is organized as follows. Section 2 describes the observational data sets used and the ozone and regressor scenarios or Monte Carlo simulations performed. Section 3 discusses the probability distributions of the explanatory power of the regressions, trends and regression values, including how the distributions depend on scenarios or Monte Carlo results. Section 4 discusses the question of detection of the second stage of ozone recovery, and in Sect. 5 a summary is given and some conclusions are drawn.

**Table 1.** Data sources.

EP flux	<a href="http://www.awi.de/en/research/research_divisions/climate_science/atmospheric_circulations_old/projects/candidoz/ep_flux_data/">http://www.awi.de/en/research/research_divisions/climate_science/atmospheric_circulations_old/projects/candidoz/ep_flux_data/</a>
QBO	<a href="http://www.geo.fu-berlin.de/met/ag/strat/produkte/qbo/">http://www.geo.fu-berlin.de/met/ag/strat/produkte/qbo/</a>
Solar flux	<a href="ftp://ftp.geolab.nrcan.gc.ca/data/solar_flux/monthly_averages/solflux_monthly_average.txt">ftp://ftp.geolab.nrcan.gc.ca/data/solar_flux/monthly_averages/solflux_monthly_average.txt</a>
SAM	<a href="ftp://ftp.cpc.ncep.noaa.gov/cwlinks/">ftp://ftp.cpc.ncep.noaa.gov/cwlinks/</a>
EESC	<a href="http://acdb-ext.gsfc.nasa.gov/Data_services/automailer/">http://acdb-ext.gsfc.nasa.gov/Data_services/automailer/</a>
Volcanic aerosol	<a href="http://data.giss.nasa.gov/modelforce/strataer/">http://data.giss.nasa.gov/modelforce/strataer/</a>
Assimilated total ozone	<a href="http://www.temis.nl/protocols/O3global.html">http://www.temis.nl/protocols/O3global.html</a>

## 2 Multivariate regression parameter uncertainties

Online data sources of the ozone observation records and applied regressors can be found in Table 1.

### 2.1 Method

A common method for analyzing total ozone records is the use of a multivariate linear regression, a method that we will use in this paper as well. The goal of the method is to attribute both inter-annual and decadal variations in the ozone record to processes that are expected or known to affect the total ozone record (Kuttippurath et al., 2013, and references therein). In the regression, the total ozone variability ( $Y$ ) as a function of time ( $t$ ) is expressed as

$$\begin{aligned}
 Y(t) &= K && \text{(Constant)} \\
 +C_1\text{HF}(t) &&& \text{(Poleward heat flux or} \\
 &&& \text{Eliassen–Palm (EP) flux)} \\
 +C_2\text{SAM}(t) &&& \text{(Southern Annual Mode index)} \\
 +C_3(\text{SF} \times \text{QBO})(t) &&& \text{(Solar flux} \times \text{QBO index)} \\
 +C_4\text{Aer}(t) &&& \text{(Stratospheric aerosol optical} \\
 &&& \text{depth)} \\
 +C_5\text{Trend}(t) &&& \text{(Total ozone trend)} \\
 +\varepsilon(t) &&& \text{(Total ozone residual).}
 \end{aligned}$$

In which  $t$  is the time from 1979 to 2010 or 2012,  $K$  is a constant and regression coefficients  $C_1$  to  $C_5$  are the regression coefficients for the respective proxies. The ozone trend ( $C_5$ ) can be related to the time-dependent equivalent effective stratospheric chlorine loading (EESC) or a PWLT before and after a predefined break year. The PWLT regressions are calculated by including two linear terms in the regression: the first term is a linear fit for the entire time window, and the second term is a linear term only for the years after a chosen break year (Kuttippurath et al., 2013).

The analysis of regression results will focus on two parameters that have previously been used in papers investigating Antarctic ozone recovery (Yang et al., 2008; Salby et al., 2011, 2012; Kuttippurath et al., 2013; Knibbe et al., 2014): the serial correlation  $R$  between the regression-based “reconstructed” ozone record and the observations, and the post-break trends and trend significance. Since the focus of our paper is to investigate trend significance, not specifically what

parameters can best explain Antarctic ozone, we will only look in some detail at the usefulness of certain regressors. However, our analysis does provide indications of which regressors are more and less useful.

In Sects. 2.2 to 2.7 the uncertainty in each of the proxies that is used as a regressor is discussed. These uncertainty ranges determine the spread in the ensemble that is used in the “big data” analysis. A summary of the regressor uncertainties and how they are incorporated in this study can be found in Table 2. The solar flux and QBO are combined into one proxy as discussed in Sect. 2.3.

### 2.2 Poleward heat flux (EP flux)

Figure 1 shows the poleward heat flux, here represented by the (vertical) EP flux (Andrews et al., 1987) at the 70 hPa level and averaged poleward of 40° S for the combined months of August and September, as well as the average EP flux available for a given year for a variety of data sets. Note that the data sets do not all completely overlap in time. Before 2000 there are considerable differences between the data sets. After 2000 these differences are smaller, which to some extent is traced to the lack of ERA-40 data beyond 2001 and lack of JRA data beyond 2004. The lower panel shows the relative differences between the five data sets and their mean. The standard deviation of all data is 7.65 %, but from 2000 onwards only 2.67 %.

Another source of uncertainty in the use of the EP flux as proxy is the choice of the time window over which the average EP flux is calculated. This choice depends on what is thought to be the relationship between variations in EP flux and ozone depletion. The basic theory states that the poleward movement of stratospheric air is proportional to the strength of the residual mean stratospheric circulation (Brewer–Dobson circulation), which in turn is driven by the poleward eddy heat flux. The poleward eddy heat flux is expressed by the upward component of the Eliassen–Palm flux that measures the upward transport of momentum by planetary waves (Andrews et al., 1987; Salby et al., 2012, and references therein). Planetary wave activity in the Northern Hemisphere affects Arctic polar vortex stability and thus Arctic ozone depletion. However, to what extent this is similar in the Southern Hemisphere is still a topic of debate. The

**Table 2.** Summary of the uncertainties for the proxies discussed in Sects. 2.1 to 2.9 and their inclusion in the regression analysis in this study.

Regressor	Variations
Average EP flux – 8 scenarios	–70 hPa, 40–90° S, August–September (baseline) – 0 hPa, 40–90° S, July–August –70 hPa, 40–90° S, July–September –70 hPa, 40–90° S, July –70 hPa, 40–90° S, August –70 hPa, 40–90° S, September –70 hPa, 45–75° S, August–September –100 hPa, 40–90° S, August–September
Solar-flux–QBO index – 100 Monte Carlo series	– Random variations in solar-flux–QBO anomalies – 200 % Gaussian noise variations on single solar-flux–QBO anomalies
SAM index – 100 Monte Carlo series	–100 % random error on annual mean SAM index values
EESC loading – 3 scenarios	– EESC shapes based on different age of air of 2.5, 4.0 and 5.5 years
Volcanic aerosol – 6 scenarios	– Baseline volcanic aerosol index (NASA GISS) – Pinatubo peak scaled to El Chichón peak – Pinatubo peak 2.5 times the El Chichón peak – Pinatubo peak 5 times the El Chichón peak – El Chichón peak shifted 1 year back compared to Pinatubo peak – Pinatubo peak shifted 1 year back compared to El Chichón peak
Ozone record – 8 scenarios	– September–October–November average ozone (baseline) – September–October average ozone – September average ozone – October average ozone – 7 September–13 October average ozone – Very short 21–30 September average ozone – Very long 19 July–1 December average ozone – “Worst” 30-day average ozone.

Arctic and Antarctic may behave either similarly (Weber et al., 2003, 2011) or not (Salby et al., 2012). This is because the notion of hemispheric similarities in how the EP flux affects ozone depletion so far is heavily based on only one outlier year (2002 for the SH, 2011 for the NH).

There are current research efforts to try to gain a better understanding of the physical and photochemical mechanisms by which the heat flux and planetary wave action affects Antarctic stratospheric ozone. A recently proposed mechanism (de Laat and van Weele, 2011) involves a pre-conditioning of Antarctic inner stratospheric vortex air whereby stratospheric temperatures affect polar stratospheric cloud (PSC) formation, which in turn affects the buildup of a halogen reservoir that later during austral spring changes the rate of catalytic ozone destruction. This preconditioning mechanism explains some years with anomalous ozone depletion, but not all. For example, during austral winter 2013 the Antarctic vortex remained largely undisturbed – oppo-

site to 2010 and 2012 (see de Laat and van Weele, 2011, and Klekociuck et al., 2011) – thus allowing for widespread PSC formation and pre-conditioning the inner vortex air for efficient ozone depletion. However, from the start of austral spring 2013 (mid-August) onwards the Antarctic stratospheric vortex got disturbed by planetary wave activity. As a result, the amount of springtime ozone depletion remained below what has been experienced during previous years with similar preconditioning. This suggests that there are multiple pathways as well as complicated interactions between chemistry and physics that can lead to reduced Antarctic springtime ozone depletion. Hence, it is unclear which regressor or regressors could act as proxies for these complex processes.

A further complicating factor is the disintegration of the Antarctic vortex, which is again controlled by planetary wave activity (Kramarova et al., 2014). The stability of the vortex determines how long the ozone-depleted inner-vortex air remains intact after photochemical ozone depletion ceases dur-

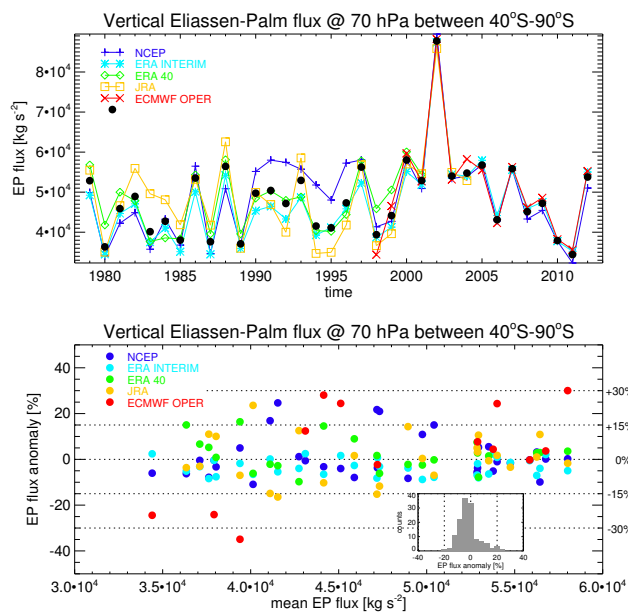


**Figure 1.** Vertical Eliassen–Palm (EP,  $\text{kg s}^{-2}$ ) flux at 70 hPa between 40 and 90° S for five different meteorological data sets for the period 1979–2012 averaged for the 2-month period August–September: NCEP reanalysis 1979–2012, ECMWF ERA-Interim 1979–2012, ECMWF ERA-40 1979–2001, Japan Reanalysis 1979–2005 and ECMWF operational analysis 1998–2012. The top panel shows the EP flux as function of time, including the mean EP flux for each year based on all data sets. The bottom panel shows the EP flux anomalies (%) of a given year as a function of the mean EP flux (black dots in the upper panel) for all meteorological data sets available for that year. The insert shows the probability distribution of the relative anomalies. Data are obtained from the EP flux data website of the Alfred Wegener Institute (AWI) for Polar and Marine Research in Bremerhaven, Germany.

ing austral spring. Variations in the duration of Antarctic vortex stability introduce variations in the Antarctic total ozone record which are not related to variations in photochemistry.

We attempt to reflect these issues in our uncertainty range for the proxy used to account for the EP flux variations in multivariate regressions. Salby et al. (2011, 2012) and Kutippurath et al. (2013) use the August–September mean EP flux poleward of 40° S and at the 70 hPa level, the baseline also used in this study. Weber et al. (2011) uses the 100 hPa poleward heat flux rather than the 70 hPa heat flux and the average over the region between 45 and 75° S rather than between 40 and 90° S. They further show that there is no particular favorable wintertime month or period from the perspective of Antarctic springtime ozone depletion over which to average the EP flux. Hence there is a certain arbitrariness involved in selecting the optimum EP flux averaging period and region.

For our study we define eight different EP flux scenarios, using different periods, latitudes and heights (see Table 2), all based on the ECMWF ERA-Interim data set. With the same

exercise as in Fig. 1 performed for these eight scenarios, the standard deviation of the EP flux time series is 21.5 %. This is considerably larger than the variability among the same EP fluxes of the different reanalysis data sets discussed above. Thus, the uncertainty in EP flux estimates largely originates from using different periods, latitudes and/or heights for which the EP flux is calculated, rather than in the use of different reanalysis data sets to calculate the same EP flux.

### 2.3 The mixed solar–QBO index

In Kutippurath et al. (2013) the effects of solar variability and QBO variability are combined into one proxy. As explained in Holton and Tan (1990), in studying high-latitude variability and trends the QBO and solar effects cannot be considered separately. Whereas the solar influence modifies tropical stratospheric ozone and dynamics, the transport of the solar signal to higher/polar latitudes depends on the phase of the QBO. As a result, solar effects on winter polar Antarctic stratospheric temperatures also depend on the phase of the QBO. If the QBO is westerly (easterly), stratospheric temperatures vary in phase (out of phase) with solar activity. It has been proposed by Haigh and Roscoe (2006) and Roscoe and Haigh (2007) to combine the QBO and solar activity into a new regression index that takes this effect into account:

$$\text{Solar-QBO index} = (\text{Solar} - S_m) \times (\text{QBO} - Q_m),$$

in which  $S_m$  is the mean of the solar flux and  $Q_m$  the midpoint of the QBO range. However, as Roscoe and Haigh (2007) note, this new index is rather sensitive to the choice of  $S_m$  and  $Q_m$ , in particular as the index is by construction the product of two anomaly fields, and thus sensitive to sign changes. In addition, the choice of  $S_m$  and  $Q_m$  is also arbitrary. Roscoe and Haigh (2007) solve this by selecting averages for which the best total ozone column regression results are obtained. However, the best regression results may not necessarily mean that the regressor is the best representation of the underlying physical mechanism, in particular as regression results also depend on other proxies and in principle there can be a cancelation of errors from different proxies in the regression. Thus, the sensitivity of the combined solar–QBO index on the calculation method of the anomalies must be further investigated.

Figure 2 shows the resulting solar-flux–QBO index time series, given various assumptions in its calculation. Clearly there is a considerable variability in the index values. The lower plot shows that the variability for every single anomaly varies by  $\pm 200\%$ . This is rather large compared to the estimated uncertainties in both individual solar flux and QBO proxies. Hence, using a combined solar-flux–QBO proxy introduces a considerable amount of additional uncertainty. For the uncertainty range in our regressions we construct 100 Monte Carlo time series in which, for each single solar-flux–

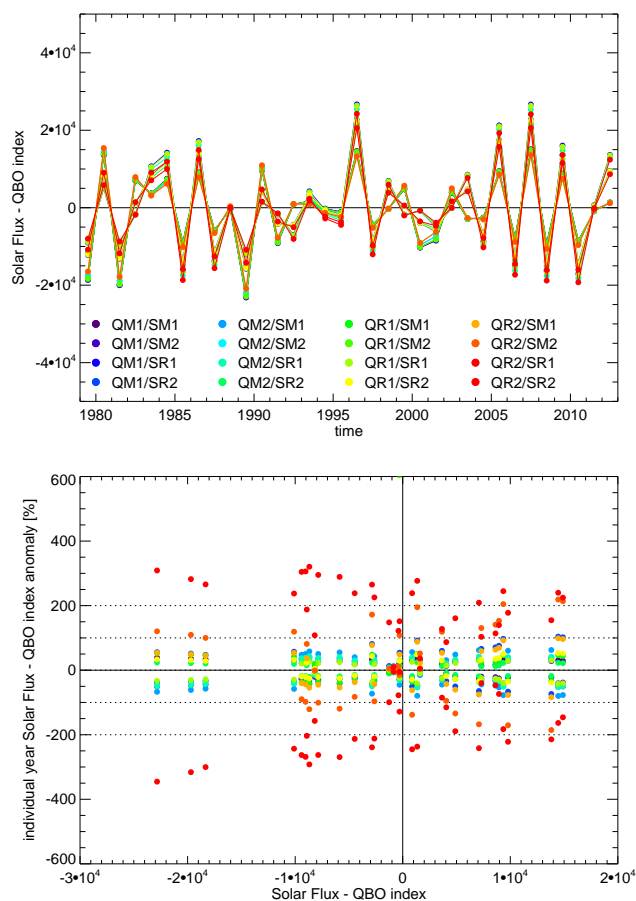


**Figure 2.** Time series of the combined solar-flux–QBO index (arbitrary units) (upper plot) and the index anomalies relative to the average of different possibilities to derive at the index. The solar flux (“S”) and QBO (“Q”) anomalies were calculated based both on the average (“M”) as well as the range of solar flux and QBO values (“R”; see section 2.5 for the explanations of the “range”), and for both the entire record of solar flux and QBO values (1947–2012 and 1953–2012, respectively; “1”) as well as for the period 1979–2012 (“2”), resulting in a total of 16 combinations. The different colors denote the different combinations.

QBO index value, random Gaussian noise is added with an amplitude of 200 % of the index value.

Note that the uncertainties in the individual QBO and solar flux proxies are much smaller than the uncertainty in the combined solar-flux–QBO index, which is relevant for high-latitude trends (see supplementary information for a separate discussion of the solar flux and QBO index).

## 2.4 Southern annular mode

The Southern Annular Mode (SAM) is a widely used index that reflects the zonal symmetry of the tropospheric circulation in the Southern Hemisphere. The symmetry of the Southern Hemisphere circulation has long been identified as an important mode of variability of the Southern Hemisphere

climate. A positive index is characterized by anomalously high surface pressure at midlatitudes and anomalously low surface pressure at latitudes closer to Antarctica.

The SAM used in this study is derived from the National Oceanic and Atmospheric Administration (NOAA). It is based on empirical orthogonal functions (EOF) applied to the monthly mean National Centers for Environmental Prediction and National Center for Atmospheric Research (NCEP/NCAR) reanalysis (Kalnay et al., 1996) 700 hPa height anomalies poleward of 20° S for the Southern Hemisphere, with the seasonal cycle being removed. The monthly SAM index is constructed by projecting the daily and monthly mean 700 hPa height anomalies onto the leading EOF mode. Both time series are normalized by the standard deviation of the monthly index (1979–2000 base time period). Since the leading pattern of SAM is obtained using the monthly mean height anomaly data set, the index corresponding to each loading pattern becomes 1 when it is normalized by the standard deviation of the monthly index.

However, there is no unique SAM index due to the existence of different meteorological data sets and different methods to quantify the symmetry of the Southern Hemisphere circulation. Kuttippurath et al. (2013) use the Antarctic Oscillation (AAO) index, which is in fact a certain choice of SAM index. A study by Ho et al. (2012) provides a comprehensive analysis of eight different SAM indices. Their analysis shows that the correlation ( $R^2$ ) between the indices varies between 0.45 and 0.96 for seasonal values and 0.73 and 0.96 for monthly values. This corresponds with random (Gaussian) variations between 20 and 100% (root-mean-square value). For most of the indices the correlation is better than 0.75. As a point of reference, adding random Gaussian noise of 50 % to a time series of a parameter and calculating its correlation with the original time series results to a correlation ( $R^2$ ) of almost 0.8.

For the uncertainty analysis we construct 100 Monte Carlo time series in which, for each single SAM index value, Gaussian noise is added with – to be on the conservative side – an amplitude of 100 % of the index value.

## 2.5 EESC loading

Uncertainties in the estimates of the EESC loading originate from two factors: the mean age of air, which reflects how fast stratospheric halogen concentrations decline due to transport velocity of halogen-poor tropospheric air from the tropical stratosphere to the polar stratosphere, and the so-called “fractional release”, the rate at which ozone-depleting substances (ODSs) release chlorine and bromine in the stratosphere. ODSs typically have not yet been dissociated when they enter the stratosphere at the tropical tropopause, and thus have fractional release values of zero. After transiting through the upper stratosphere, the ODSs in an air parcel become fully dissociated due to their exposure to energetic radiation and

the fractional release values get close to 1.0 (Newman et al., 2007).

To complicate matters, the mean age of air in the stratosphere is not a constant but varies with latitude, height and season (Stiller et al., 2008). On average, the age of air increases with height, i.e., it takes longer for tropospheric air to travel higher in the stratosphere, and the age of air also increases towards the poles because of the time it takes for air to travel from the tropical “source” region to higher latitudes. In the Antarctic vortex regions there is a strong seasonal dependence of the age of air due to the isolation of inner vortex air during austral winter and spring, while upper stratospheric and mesospheric air slowly descends in the Antarctic vortex. The descending air is particularly “old” air and causes strong vertical gradients in the age of air in the wintertime polar vortex. Stiller et al. (2008; their Fig. 7) show that the age of air almost triples going up from 15 km ( $\theta = 400$  K; age of air  $\sim 4$  years), to 20 km ( $\theta = 400$  K; age of air  $\sim 7$  years), to 25 km ( $\theta = 600$  K; age of air  $\sim 9$  years), to finally 30 km ( $\theta = 750$  K; age of air  $\sim 11$  years). How to account for this variability in a regression is unclear, but it is unlikely that one age-of-air value can be attributed to the total ozone column.

Moreover, ozone variability in the Antarctic vortex is determined by different processes at different altitudes. Halogen-related ozone depletion typically maximizes between 15 and 20 km altitude ( $\sim 100$ – $50$  hPa, US Standard atmosphere 1976;  $\theta = 400$ – $500$  K), whereas the effect of vortex stability on ozone depletion is seen predominantly between 20 and 30 km altitude ( $\sim 50$ – $10$  hPa;  $\theta = 500$ – $750$  K) (de Laat and van Weele, 2011). Thus, total ozone column observations which are vertically integrated amounts of ozone are being affected by different processes at different altitudes.

The age of air may also not be constant over the time period over which ozone trends are determined. Due to a changing climate the stratospheric circulation may speed up (e.g., Engel et al., 2009; Bunzel and Schmidt, 2013), causing a decrease in the age of air with increased warming, which obviously then depends on the exact warming. This introduces yet another uncertainty for the periods from 1979 to 2010 or 2012 that are considered in this study.

The age-of-air uncertainties do not manifest themselves as a random process, which would make it useful for applying a Monte Carlo method, but as a structural uncertainty, i.e., the entire EESC shape would change for different parameter settings. Such uncertainty could be captured by applying a parametric bootstrap rather than a Monte Carlo approach. However, such a parametric approach would also not suffice because we use total column observations and we know that ozone at different altitudes would be affected by different parameter values.

A pragmatic approach with regard to the sensitivity of the regression to EESC values is testing the robustness of the regression results as a function of the assumed EESC time evolution. For the uncertainty analysis we assume three different

EESC scenarios with an age of air of 2.5, 4 and 5.5 years and a half-width of 1.25, 2 and 2.75 years, respectively. The largest differences between the three scenarios are in their post-peak trend in EESC (see later on in Fig. 3).

## 2.6 Volcanic aerosol

Aerosols from sufficiently strong volcanic eruptions can reach the stratosphere and affect stratospheric ozone chemistry. In particular strong eruptions occurring in the tropics can have long lasting effects on stratospheric ozone. Aerosols reaching the tropical stratosphere are slowly transported towards middle and high latitudes. It can take up to a decade before the stratosphere is cleared from volcanic aerosols (Vernier et al. 2011; Solomon et al., 2011). Volcanic eruptions at middle and high latitudes have much shorter lasting effects. These aerosols enter in the descending branch of the stratospheric circulation and will be relatively quickly removed from the stratosphere.

The short-term effect of stratospheric volcanic aerosols is heating of the stratospheric layer, which affects stratospheric ozone in the tropical belt. The dominant long-term effect of stratospheric volcanic aerosols on global and polar ozone is, however, the increase in aerosol surface area density and subsequent heterogeneous ozone loss. Model simulations of volcanic aerosol effects on stratospheric ozone suggest that, in particular under cold conditions (high-latitude, wintertime, lower stratosphere), total ozone columns can be reduced by up to 10–15 % (Rozanov et al., 2002). During other seasons, total ozone column depletion by volcanic aerosols is of the order of a few percent.

Since 1979 two major tropical volcanic eruptions have affected stratospheric ozone: El Chichón, Mexico, in 1982, and Pinatubo, Philippines, in 1991. Although the total amount of stratospheric aerosols by both eruptions has been characterized relatively well, there appear to be considerable uncertainties associated with the time evolution of the aerosol amounts in the Southern Hemisphere. A brief and incomplete survey of a latitudinal volcanic aerosol radiative forcing data record (Ammann et al., 2003) and a global volcanic aerosol proxy record (Crowley and Unterman, 2012) as well as the standard volcanic aerosol index used in Kutippurath et al. (2013) – aerosol optical depth (Sato et al., 1993; updates available via NASA GISS) – all show that there are large differences between the El Chichón aerosol peak relative to the Pinatubo peak. Large differences are seen in global, hemispheric and Southern Hemisphere (Antarctic) aerosol amounts as well as differences in the exact timing of the peak aerosols (Sato et al., 1993; Ammann et al., 2003; Crowley and Unterman, 2012). The El Chichón aerosol peak relative to the Pinatubo peak for high Antarctic latitudes can be similar (Ammann et al., 2003), about 3 (Sato et al., 1993) to (globally) 8 times smaller (Crowley and Unterman, 2012). The Pinatubo peak aerosol in the Southern Hemisphere was

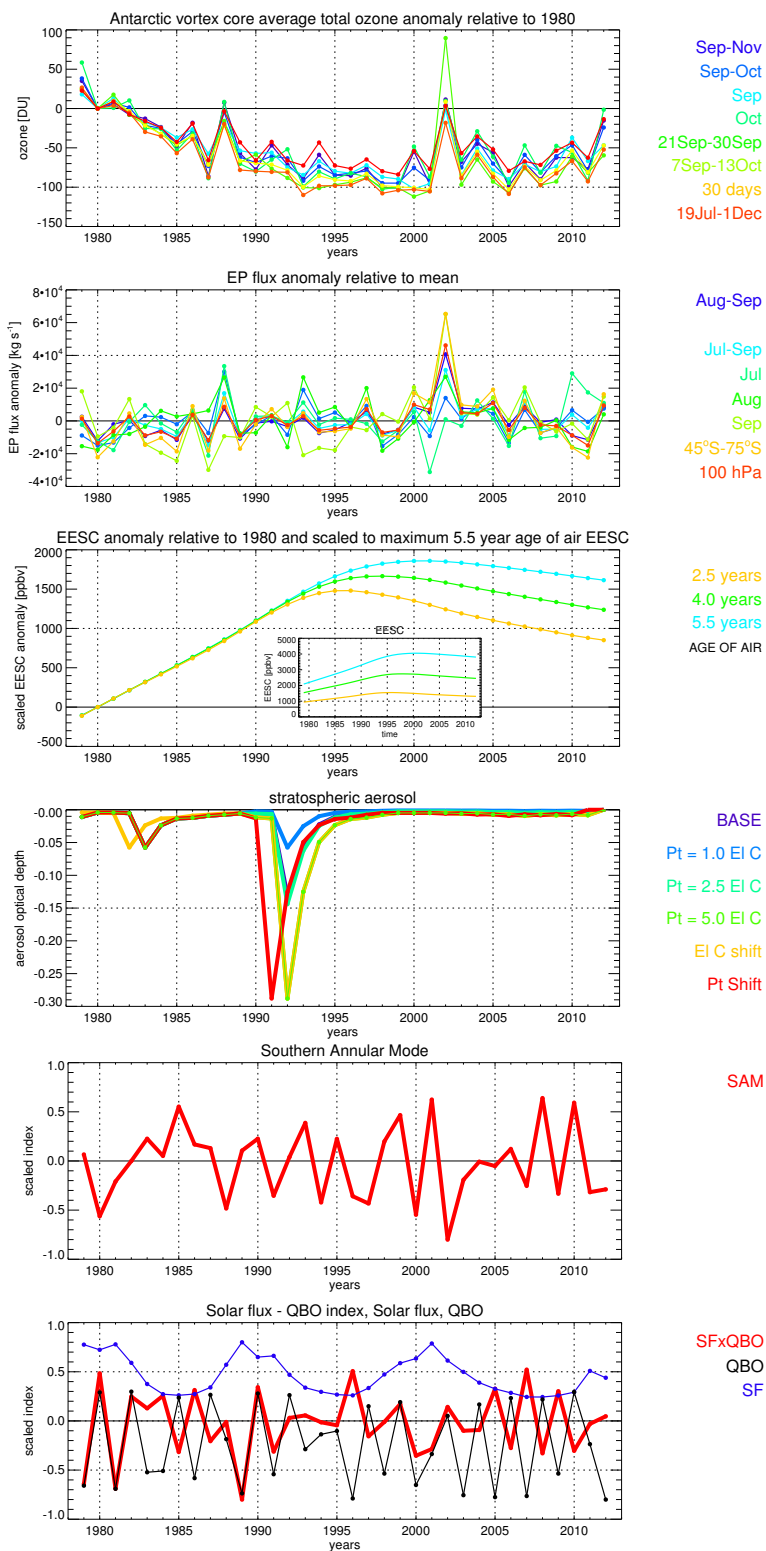


**Figure 3.** Time series of regressors for the period 1979–2012. For ozone, EP flux, EESC and stratospheric aerosol, all scenarios as defined in Sect. 2 are included (indicated by the different colors). For the SAM and the solar-flux–QBO index only the baseline time series is shown, and both indices – being unitless to start with – are scaled for proper comparison. Ozone values are in DU, EP fluxes are in  $\text{kg s}^{-1}$ , EESC values are in ppbv and stratospheric aerosol is in optical depth.

about half the size of the global-mean Pinatubo peak (Ammann et al., 2003).

Kuttippurath et al. (2013) shift the Southern Hemisphere aerosol data by 6 months to account for the transport of aerosols. Although they report that the 6-month shift results in the best statistics, the analysis presented in the previous paragraph shows that the effect of the shift is relevant for the shape of the volcanic aerosol changes, but does not introduce variations as large as the other variations in volcanic aerosol indices. Given that a time shift is included in the six volcanic aerosol scenarios defined above, we do not add additional time shifts in the aerosol record.

We define six volcanic aerosol scenarios that reflect the uncertainty in the volcanic stratospheric aerosol records. The base scenario is the scenario used in Kuttippurath et al. (2013), which in turn uses the NASA GISS stratospheric aerosol record. A second scenario is with the Pinatubo aerosol curve scaled so that the maximum matches the El Chichón aerosol peak, the Pinatubo curve maximum is 2.5 times the El Chichón peak, and the Pinatubo curve maximum is 5 times the El Chichón peak. The uncertainty in timing of the Southern Hemispheric aerosol peak is considered by a shift of the El Chichón peak 1 year back compared to the Pinatubo peak and a shift of the Pinatubo peak 1 year back compared to El Chichón peak.

## 2.7 Ozone scenarios

It is a priori unclear what would be the most appropriate ozone scenario to use in the regression. Both Salby et al. (2011, 2012) and Kuttippurath et al. (2013) use the September–November 3-month averaged total ozone record. However, as discussed in the introduction, different processes affect ozone during different time periods. Studies in the literature use very different time periods for averaging ozone to investigate Antarctic ozone trends. We define eight different ozone scenarios to reflect the ozone records used in the literature (see also de Laat and van Weele, 2011), using the MSR data set (van der A et al., 2010). The MSR is a 30-year total O<sub>3</sub> column assimilation data set for 1979–2008 based on a total of 11 satellite instruments measuring total O<sub>3</sub> columns – including SCIAMACHY – that were operating during various periods within these 30 years. For the period 2009–2012 the MSR data set was extended with assimilated SCIAMACHY and GOME-2 total ozone column data. Apart from the September–November 3-month averaged total ozone record we also use averages of total ozone over the month of September, the month of October, the 2-month period September–October, a very long period (19 July–1 December), a very short 10-day period (21–30 September), the period 7 September–13 October, and a year-dependent “worst” 30-day period (30-day average with the largest ozone mass deficit).

## 2.8 Other uncertainties

Kuttippurath et al. (2013) address two other important uncertainties for the determination of the ozone trend. First, the area over which the ozone record is defined (inside vortex, equivalent latitude 65–90° S, and vortex core). The area is important for the absolute amounts of ozone depletion, but Kuttippurath et al. (2013) show it is much less relevant for the differences in trend. That is, the uncertainties in the estimated linear trend dominate the uncertainties due to different areas over which the ozone anomalies are calculated. A second uncertainty on their ozone trend derives from the use of different ozone data sets (ground-based, TOMS/OMI and MSR). Here the uncertainties in the estimated linear trend also dominate the uncertainties due to the different data sets. Hence, we do not include these uncertainties in our analysis.

In addition, there are many studies trying to identify the moment when ODSs stop increasing and/or when ozone stops decreasing. The maximum ODSs appears somewhere between 1997 and 2000 (Newman et al., 2007), depending on geographical location and height. However, due to saturation effects – there are more than sufficient ODSs present to destroy all Antarctic ozone between 15–20 km altitude – the moment where ozone starts to be affected by decreasing ODSs may actually be later (Kuttippurath et al., 2013; Kramarova et al., 2014).

The moment of a structural break in ozone based on observations indicates an early break around 1997 (Newchurch et al., 2003; Yang et al., 2008). However, some processes affecting stratospheric ozone vary on long timescales – solar effects and volcanic eruptions come to mind – which may affect the observation-based analysis of break points (Dameris et al., 2006). Note that we confirm this break year of 1997 based on applying a break-point analysis algorithm to the MSR ozone record (not shown). Hence, we decided to use three different break years that have been identified and/or are most commonly used: 1997, 1998 and 1999.

## 2.9 Selected uncertainty ranges and ozone record scenarios

Figure 3 shows the baseline regressor time series and the scenarios for ozone, the EP flux, EESC loading and volcanic aerosols. A total of 100 different solar-flux–QBO index and SAM index time series are used to span their uncertainty range (not shown in Fig. 3). All scenarios and Monte Carlo results combined provide 11.5 million different choices for the regressions ( $100 \times 100 \times 8 \times 8 \times 6 \times 3$ ; see Table 2). Ozone trends are calculated based on the EESC loading or using a PWLT analysis. For the PWLT ensembles the three different EESC scenarios are irrelevant. Instead, the sensitivity of the regressions is tested using three different break years (1997, 1998 and 1999). In total we analyze approximately 23 million different trends using the EESC and PWLT scenarios.

**Table 3.** EESC-based Antarctic vortex core ozone trends and their  $2\sigma$  trend uncertainties ( $\text{DU year}^{-1}$ ) derived from multivariate linear regression. The trends in ozone based on EESC regression are calculated by means of an ordinary linear regression based of the pre-defined change in EESC multiplied by the EESC regression coefficient for the time period under consideration (cf. Kuttippurath et al., 2013). The EESC trend is in  $\text{pptv year}^{-1}$ , the EESC regression coefficient is in  $\text{DU pptv}^{-1}$ , and hence the trend in ozone is in  $\text{DU year}^{-1}$ , allowing direct comparison with the PWLT ozone trends (also in  $\text{DU year}^{-1}$ ).

Period	Kuttippurath et al. (2013)		This study	
	EESC	PWLT	EESC	PWLT
1979–1999	$-4.50 \pm 0.65$	$-5.02 \pm 1.11$	$-5.39 \pm 0.22$	$-5.66 \pm 1.03$
2000–2010	$1.11 \pm 0.16$	$2.91 \pm 2.73$	$1.04 \pm 0.12$	$3.30 \pm 2.85$
1979–1999			$-5.26 \pm 0.21$	$-5.75 \pm 1.00$
2000–2012			$1.09 \pm 0.10$	$3.28 \pm 2.49$

Note that by basing our analysis on both different ozone and EP flux scenarios, certain time-lag relations are taken into account. It should also be noted that the use of such a wide range of scenarios indicates that much remains unclear about what best describes Antarctic ozone depletion and the time-lag relations between ozone and explanatory variables.

### 3 Scenario analysis

#### 3.1 Reproducing Kuttippurath et al. (2013)

First a multivariate regression similar to Kuttippurath et al. (2013) is performed in which the MSR data set is used within the vortex core ( $70\text{--}90^\circ\text{S}$ ). The results are summarized in their Fig. 5 and Table 4, which are duplicated here in Table 3 along with the results from a multivariate regression based on the same variables as used in Kuttippurath et al. (2013).

Our results reproduce the results from Kuttippurath et al. (2013), although there are minor differences in the absolute numbers, most likely related to differences in EP fluxes (Jayanarayanan Kuttippurath, personal communication, September 2013). The trends for the periods 1979–1999 and for 2000–2010 are of comparable magnitude in both studies, as well as the PWLT significance levels for the period 1979–1999 and the EESC trends for both 1979–1999 and 2000–2010. The magnitude of the recovery for 2000–2010 based on the PWLT is slightly larger, but also in our analysis the post-2010 linear trend in ozone is significant beyond  $2\sigma$ . For the correlation of the regression model with the ozone record, we obtain a value of 0.87 ( $R^2$ ) comparable to the 0.90 ( $R^2$ ) reported in Kuttippurath et al. (2013). Thus, the results are sufficiently similar to proceed with studying the effects of the uncertainties in regressors and ozone record scenarios on the regression results. Note that we calculate the pre-break and post-break EESC-based trends by applying linear regressions to the EESC curve multiplied with the EESC regression coefficient for the pre-break and post-break time periods. As a result, EESC-based trend errors are related to the nonlinearity of the EESC curve, and the trend errors differ for both

the pre-break and post-break time periods. Our EESC-based trend errors differ from those in Kuttippurath et al. (2013), which lacks a description of how EESC-based trend errors are calculated.

#### 3.2 Ozone record and regressor correlations

Before analyzing the ensemble of regression results it is important to investigate the correlations between the different regressors. If correlations between regressors are too large, they cannot be considered to be independent, and it should be decided which one to omit from the analysis, as the regression otherwise cannot separate which variability is related to which regressor. Furthermore, it is a priori useful to understand how regressors correlate with the ozone record, as a small correlation implies that a regressor can only explain a limited amount of ozone variability.

Table 4 shows the mean correlation between the different regressors and their  $2\sigma$  spread based on the ozone record and regressor selections and/or Monte Carlo results (SAM,  $\text{SF} \times \text{QBO}$  index). The EP flux correlates positively with the EESC and negatively with the SAM and, to a lesser extent, also with the  $\text{SF} \times \text{QBO}$  index. The other regressors do not show significant cross-correlations. Only for a few individual ozone record scenarios are cross-correlations found to exceed 0.5.

The uncertainty in the correlations with the ozone records ranges between about 10 and 20 % for each of the regressors. Small cross-correlations between the regressors, however, do not provide a justification for a priori omitting one of the regressors.

#### 3.3 Trends

Figure 4 shows the probability distributions of the ozone trends for 1979– $Y_B$  and  $Y_B$ –2012 periods, in which  $Y_B$  is the break year, which can either be 1997, 1998 or 1999. For the 1979– $Y_B$  period the mean EESC trend is  $-5.56 \text{ DU year}^{-1}$  ( $-4.00$  to  $-7.06$ ; 95 % CI) and the mean PWLT trend is  $-6.40 \text{ DU year}^{-1}$  ( $-4.22$  to  $-7.18$ ; 95 % CI). For the  $Y_B$ –2012 period the mean EESC trend is  $+1.97 \text{ DU year}^{-1}$

**Table 4.** Cross correlations and their  $2\sigma$  variance between explanatory variables.

	EPFLUX	EESC	AEROSOL	SF $\times$ QBO
SAM	$-0.31 \pm 0.27$	$-0.03 \pm 0.17$	$-0.09 \pm 0.19$	$-0.09 \pm 0.29$
SF $\times$ QBO	$0.08 \pm 0.28$	$0.07 \pm 0.42$	$-0.02 \pm 0.19$	
AEROSOL	$0.05 \pm 0.17$	$0.03 \pm 0.30$		
EESC	$0.25 \pm 0.17$			

( $+0.84$  to  $+3.32$  DU year $^{-1}$ ; 95 % CI), and the mean PWLT trend is  $+3.18$  DU year $^{-1}$  ( $+1.66$  to  $+4.74$ ; 95 % CI).

For the 1979– $Y_B$  period the distributions of EESC and PWLT trends (top panel) are rather similar, although the PWLT correlations show a larger peak towards high correlations compared to the EESC correlations (bottom panel). However, for the  $Y_B$ –2012 trends the probability distributions are very different (middle panel). The EESC trends show a trimodal distribution, because only three different EESC curves were used. These three EESC curves differ predominantly in their post-1997 EESC trends (see also Fig. 3). In addition, the trimodal EESC trend probability distribution for  $Y_B$ –2012 (middle panel) shows that the EESC fit in the linear regression is determined by the 1979– $Y_B$  period more than by the  $Y_B$ –2012 period, as the pre-break trend distribution does not show the same trimodal shape. This is not surprising because the trends for the 1979– $Y_B$  period are larger and cover a longer period than for  $Y_B$ –2012.

The correlations distributions (lower panel) are similar for the lowest and highest correlations for both the EESC and PWLT regressions, but in the bulk of the distribution the PWLT results in systematically higher correlations than the EESC regressions.

The upper two panels of Fig. 4 also include the 1979–1999 and 2000–2012 PWLT trends and  $2\sigma$  errors as reported in Table 2. The uncertainty range of the 2000–2012 PWLT trend in Table 2 and the range in Fig. 4 are quite similar. However, the uncertainty range of the 1979–1999 PWLT trend in Table 2 is considerably smaller. This shows that uncertainties in the 1979–1999 ozone trends are larger than estimated using a single regression estimated even though all 1979–1999 trends are statistically significant.

The autocorrelation of the ozone residuals is small (1-year lag values are approximately zero), indicating that the autocorrelation present in the ozone record (e.g., Fioletov and Shepherd, 2003; Vyushin et al., 2007) is related to some of the processes described by the regression parameters and are removed by the multivariate regression. Auto-correlation thus does not have to be taken into account in the trend significance calculation.

### 3.4 Regression model performance: sensitivity to the independent variables

Sensitivities of the PWLT-based and EESC-based regressions to the ozone and EP flux scenarios are shown in Fig. 5.

PWLT-based regressions show that the PWLT distribution peak at high correlations is a consistent feature of different ozone records (September–November, September–October, Sep, 7 September–13 October, worst 30 days). Similarly, use of several different EP fluxes also aligns with the PWLT correlation distribution peak, in particular the EP flux scenarios that include both August and September. For ozone, correlations get smaller for the longest period (19 July–1 December), shortest period (21–30 September) and October averages.

Figure 6 shows the probability distribution of volcanic aerosols for both the PWLT and EESC regressions. Volcanic aerosols have little impact on the explanatory power of the regression results, as already indicated by lack of correlation of this regressor with the ozone record. The PWLT regression coefficient values show that the effect of volcanic aerosols on ozone can be either positive or negative, largely depending on the assumed amount of Pinatubo aerosols relative to El Chichón aerosols, although the distribution predominantly suggests positive regression values. The EESC regressions show a similar sign dependence of ozone on volcanic aerosol, but with no clear sign of the regression value. None of the other parameters (EPFLUX scenario, ozone scenario) have a sign-dependent effect on the aerosol regression coefficient value for both the EESC and PWLT scenarios. The strong sensitivity of the volcanic aerosol regression value – including sign changes – to either aerosol or EESC scenario indicates that including volcanic aerosols is not very important for the multivariate regression and is best excluded altogether from multivariate regressions due to insufficient information in the Antarctic ozone record to constrain the ozone–volcanic-aerosol relation.

For the solar-flux–QBO index (Fig. 7a) we find no clear dependence of regression coefficient values on any of the scenarios or parameters. The probability distributions for both the EESC and PWLT regressions are very similar. Hence, like for volcanic aerosols, the solar–QBO parameter better should be excluded altogether from multivariate regressions because the Antarctic ozone record probably contains insufficient information to constrain the ozone–solar–QBO relation.

The SAM regression coefficient values show a continuous random distribution, while the overall dependence is predominantly negative (Fig. 7b). A positive phase of the SAM correlates with more ozone depletion than a negative phase of the SAM. This is a well-known two-way effect: tropospheric

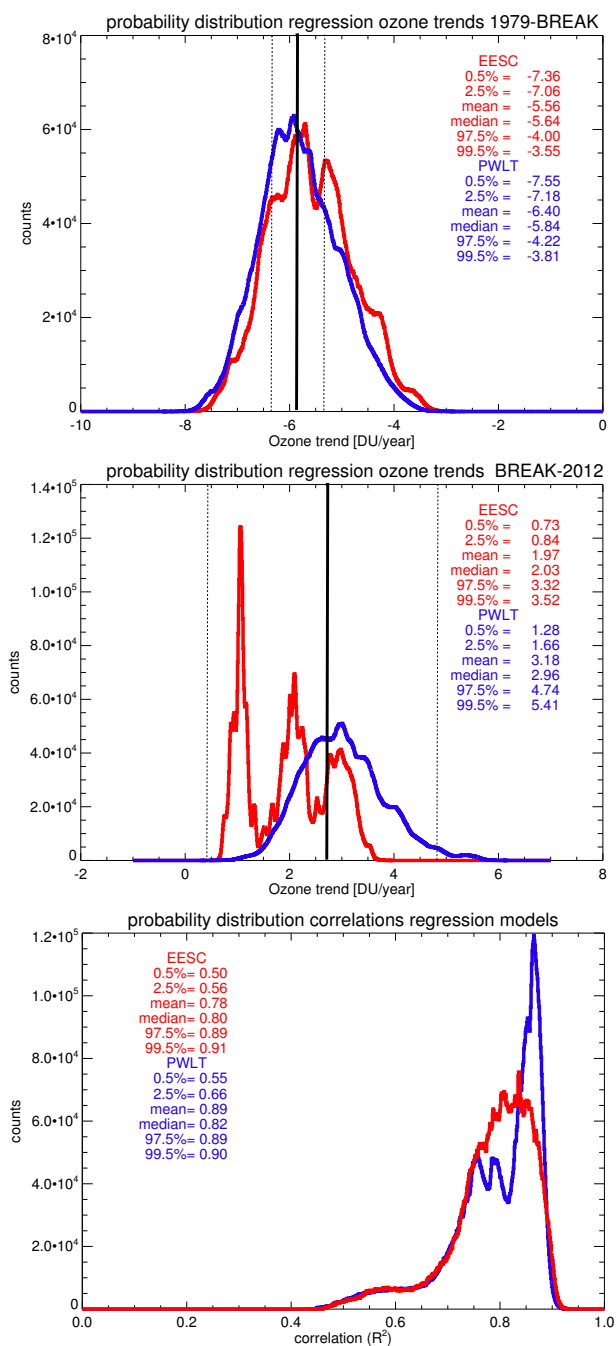


**Figure 4.** Probability distribution of ozone trends for the period 1979-break (upper plot) and break-2012 (middle plot) as well as time correlations ( $R^2$ ) for the regression models and the ozone record scenarios (lower plot). The colors indicate the distributions for the two different long-term ozone regressions (EESC, PWLT). Indicated in the figure are also the 0.5 %, 2.5 %, mean, median, 97.5 % and 99.5 % probability values of trends and correlations. The vertical black lines in the upper two panels indicate the trend (solid) and  $2\sigma$  errors (dotted) of the PWLT regression results of Table 2 for the period 2000–2012.

circulation changes affect Antarctic stratospheric ozone on the short term, while the long-term changes in Antarctic ozone have affected the tropospheric circulation in the Southern Hemisphere (Kirtman et al., 2013; IPCC AR5, Ch. 11, Sect. 11.3.2.4.2, and references therein).

For the EPFLUX, the regressions show a positive dependence (Fig. 7c) and a similar distribution for both the EESC and PWLT regression.

### 3.5 Optimal regressor and ozone record scenarios

Based on the analysis of the entire ensemble presented here, it might be possible to choose an optimal set of regressors as well as an optimal ozone record scenario for Antarctic ozone trend analysis. Volcanic aerosols (Fig. 6), the QBO and the solar cycle (Fig. 7) are shown to have little effect on the regression and thus are best excluded. For the EP flux, it appears that including the months August and September leads to a better fit (higher correlations; Tables 4 and 5, Fig. 5). For ozone, results suggest that there is no clear optimal time window over which to calculate average ozone, but it appears that the period should not be too short or too long, and should include September and preferably the first half of October (Tables 4 and 5).

In addition, the use of three different EESC scenarios results in trimodal distribution features in several parameters (Figs. 3 and 6), suggesting that care has to be taken with, in particular, the ozone trend values attributed to changes in EESCs. Furthermore, the post-break trends are particularly sensitive to the choice in EESC scenario (Fig. 3). It could therefore be argued that using a PWLT for post-break trend estimates is preferred over using the EESC-based post-break trend as its distribution better reflects structural uncertainties in the regression and takes the regression residuals into account for calculation of trend uncertainties.

Figure 8 illustrates what the best single regressions in the entire ensemble for all three regression models separately look like. The best EESC regression correlation ( $R^2 = 0.95$ ) was found for a case with September–November ozone, July–August EP flux and an EESC with an age of air of 4 years. For the best PWLT regression correlation ( $R^2 = 0.96$ ) these were the same with 1997 as the optimal break year. The reason for the high explanatory power is that in all three cases the SAM anomalies align with strong ozone peaks, whereas the solar-flux–QBO index variations coincidentally align with the smaller ozone anomalies.

## 4 Discussion: second stage of ozone recovery and trend significance

Given the broad range of outcomes for the different types of regressions and regressors, an important question is not only whether ozone started to increase after the late 1990s but also whether the trend is statistically significant and can

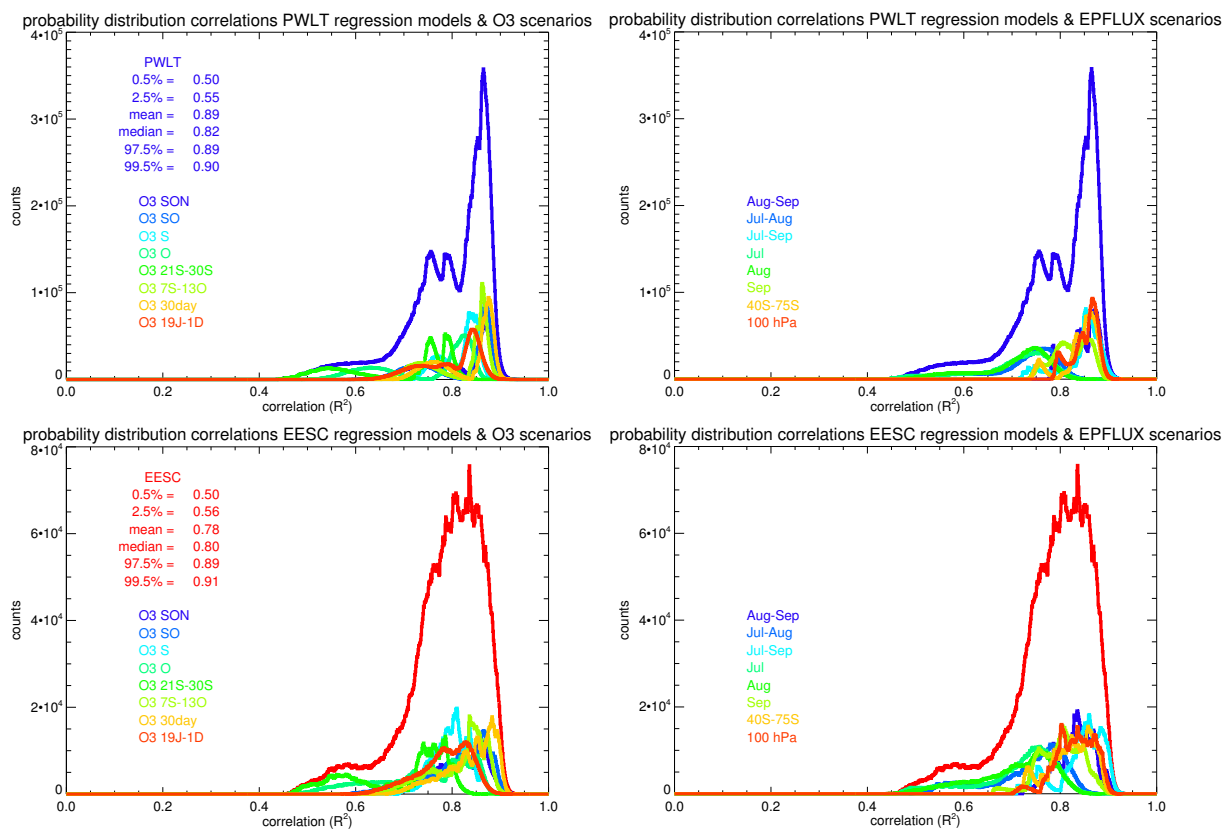


**Figure 5.** Probability distribution of regression-model–ozone-scenario correlations as Fig. 4, lower plot, for the PWLT and EESC regression model and sensitivity to the different ozone scenarios and different EP flux scenarios, indicated by the different colors. The blue and red outlines show the sum of all scenarios combined.

be attributed to declining stratospheric halogens, which is required by WMO for the second stage of ozone recovery to be formally identified. Because the EESC curve shape is prescribed, there is no degree of freedom allowing for different pre-break and post-break trends in the EESC regression. As discussed in Sect. 2, it is not clear a priori which EESC scenario is the optimal choice or if it is even appropriate to use just a single EESC scenario. Hence, how to assign overall uncertainty to the EESC curve remains an open question. Therefore, a better approach would be to investigate whether the PWLT post-break trends are statistically significant as they use the ozone fit residuals for their significance calculation.

Figure 9 shows the probability distribution of correlations ( $R^2$ ) of the PWLT regression models vs. ozone for the entire Monte Carlo data set, as well as the fraction of post-break PWLT trend estimates that are statistically significant ( $2\sigma$ ) for both the periods ending in 2010 and 2012. This figure is comparable to Fig. 4 (lower panel) and Fig. 5, but with larger correlation bins for visualization purposes. Results indicate that trends only become statistically significant beyond a certain explanatory power of the regression model. This is not

surprising: only when ozone residuals are sufficiently small after removing the regression results can the post-break trend become statistically significant. This automatically requires a high correlation between the ozone record and the selected regression model. The analysis here shows that statistically significant trends require a correlation ( $R^2$ ) of at least approximately 0.60. Furthermore, the majority of trends only become statistically significant for high values ( $R^2 > 0.80$ ) of the correlation between ozone and the regression model.

In Sect. 3.5 the results of the ensemble were analyzed to determine optimal scenarios in terms of explanatory power ( $R^2$ ). However, the second stage of ozone recovery also requires a statistically significant post-break year trend. We therefore analyzed the percentage of statistically significant post-break trends in the ensemble for the PWLT-based regressions. We focus on the ozone record and EP flux scenarios as the uncertainties associated with these two parameters are the most important ones, as discussed before. Table 5 shows the percentage of regressions for each combination of ozone record and EP flux scenarios that is statistically significant for the ozone records ending in 2010. There are large differences in the fraction of statistically significant PWLT-

**Table 5.** As Table 5 but for the break year 1997 and the period ending in 2012.

EP flux	Aug–Sep	Jul–Aug	Jul–Sep	Jul	Aug	Sep	45–75° S	100 hPa
Ozone								
Sep–Nov	99.9	10.7	92.6	0.1	36.3	29.5	100.0	100.0
Sep–Oct	100.0	52.2	100.0	4.2	73.4	100.0	100.0	100.0
Sep	100.0	40.3	99.5	2.0	67.5	96.4	100.0	100.0
Oct	100.0	12.1	98.0	0.6	27.2	98.1	100.0	100.0
21–30 Sep	< 0.1	< 0.1	< 0.1	< 0.1	< 0.1	< 0.1	< 2.0	< 20.9
7 Sep–13 Oct	100.0	10.0	97.7	0.8	19.6	98.4	100.0	100.0
Worst 30 days	100.0	20.0	99.4	1.2	29.6	99.7	100.0	100.0
19 Jul–1 Dec	99.9	25.6	95.3	1.5	66.1	56.5	100.0	100.0

**Table 6.** Fraction of statistically significant trends (%) in all regression results for different break years, period lengths and different types of trend calculations. The start year and end year refer to the time period for which trends are calculated. ‘All’ under ‘Start year’ refers to the statistics for all three start year scenarios combined.

Start year	End year	Length (years)	significant trends
2000	2010	11	34.3 %
1999	2010	12	47.8 %
1998	2010	13	59.5 %
All	2010		47.3 %
2000	2012	13	39.0 %
1999	2012	14	52.7 %
1998	2012	15	60.7 %
All	2012		50.5 %

based trends, ranging from less than 0.1 % (21–30 September average ozone) to more than 50 % significance (September ozone, October EP flux). Table 6 shows the same results as Table 5, but only for the break year 1997 and the period ending in 2012. In this case there is a large number of ozone-record–EP-flux scenario combinations with statistically significant trends. If we were to consider only the EP fluxes that include the months of August and September, then with the exception of the 21–30 September time window nearly all trends are statistically significant.

Table 7 shows that the number of significant trends further depends on the choice of break year, with the number of statistically significant trends increasing steadily with increasing length of the period over which trends are calculated. This is not surprising as the regression trend error decreases with increasing number of points for which the trends are calculated (Supplement Eq. S2).

Excluding the year 2002 from the regressions has a significant impact on the post-break ozone trends themselves. However, it hardly has any effect on the post-break trends from the regressions (not shown), indicating effective removal of the anomalous year 2002 from the results. Excluding volcanic

years from the regression had no significant effect on both the ozone trends before and after the regression, consistent with our finding that there appears to be little (direct) impact of volcanic aerosols on Antarctic springtime ozone.

It is tempting to interpret, based on some selections of our results, that the significance is sufficient for identification of the second stage of ozone recovery in the Antarctic ozone hole by 2012. However, comparison Table 5 and Table 6 – thus 2000–2010 trends vs. 1998–2012 trends – shows that the longer period does not always result in increased statistical significance. In particular, the need to average ozone over longer periods of time may introduce long-term changes in average ozone that are not related to photochemical ozone destruction. Furthermore, the trend significance of single regressions is generally between  $2\sigma$  and  $3\sigma$  (not shown), indicating that a considerable amount of variability is not accounted for in the regression. In addition, our analysis shows that detection of the second stage of ozone recovery based on just one arbitrary selected (set of) regressor–ozone-record combination(s) does not reflect the structural uncertainties present in the underlying data.

Nevertheless, the appearance of large groups of statistically significant results occurring for longer time series and a certain persistence among ozone scenarios and EP flux scenarios shows that these type of analyses are capable of removing deterministic variations in average ozone, and that more statistically significant results can be expected with increasing length of the post-break period.

## 5 Conclusions

The primary goal of this study was to investigate whether or not the second stage of ozone recovery – a statistical increase in ozone attributable to ozone-depleting substances – can be detected, given uncertainties in underlying data. A detailed sensitivity analysis of widely used multivariate regression analysis of total ozone columns was presented, focusing on Antarctic springtime ozone. By combining regressor sce-

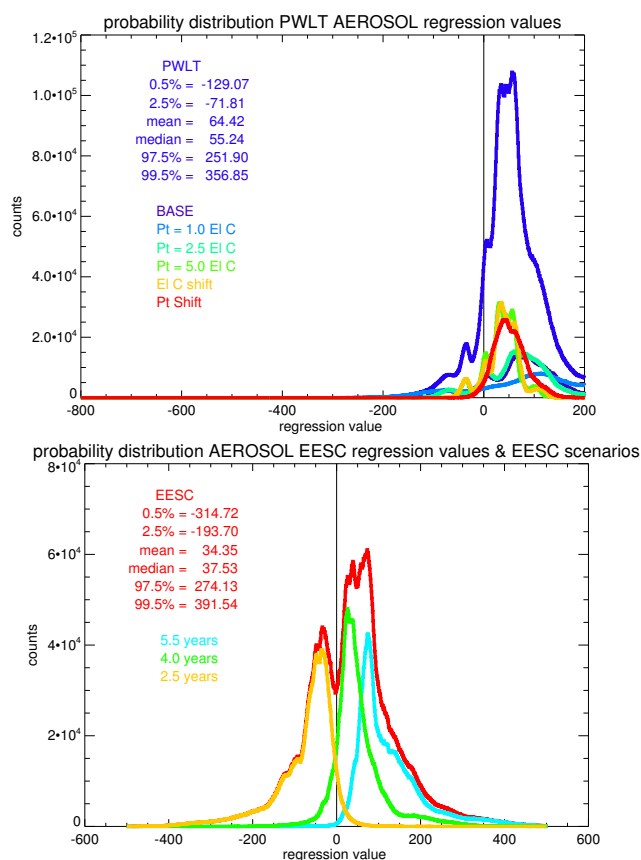


**Figure 6.** Upper panel: probability distribution of aerosol scenario regression coefficient values of all PwLT regression results. Indicated in the figure are also the 0.5 %, 2.5 %, mean, median, 97.5 % and 99.5 % probability values of trends and correlations. Included are also the distributions for the different stratospheric aerosol scenarios, indicated by the different colors. Lower panel: probability distribution of the aerosol regression coefficient values of the EESC regression model results. Included are also the distributions for the three different EESC age of air scenarios, indicated by the different colors. The blue and red outlines show the sum of all scenarios combined.

narios and Monte Carlo simulations for various ozone record scenarios, a total of approximately 23 million different multivariate regressions were performed.

Use of the post-break trends based on fitting the EESC to the total ozone record is not recommended, as these trends are solely based on the pre-defined EESC shape and do not allow for flexibility in the trend calculation. Because the resulting EESC-fit-based trend uncertainties do not take the ozone fit residuals into account, the EESC scenarios result in overconfident ozone trend uncertainties, neglecting structural uncertainties and sensitivity to the chosen scenario.

Our analysis shows that the EP flux and the SAM effects are capable of explaining significant parts of Antarctic ozone variations and the removal of these effects improves the analysis of recovery, in contrast to the inclusion of vol-

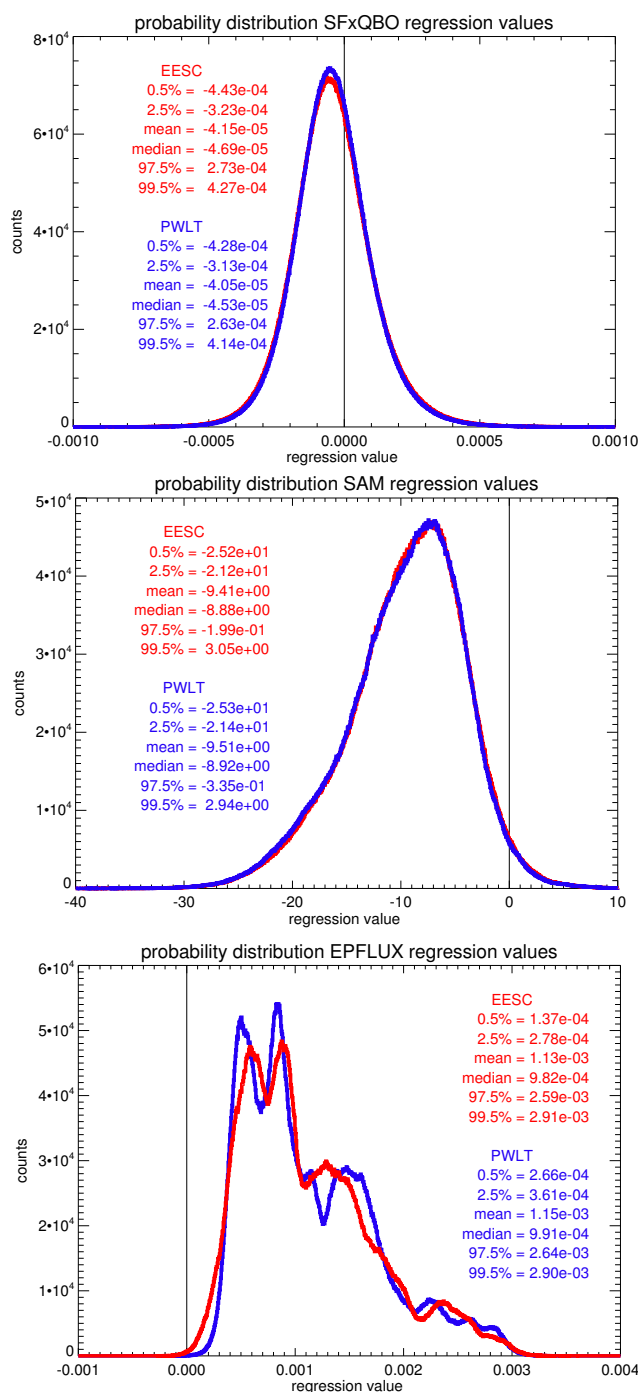


**Figure 7.** (a) Probability distribution of the solar-flux–QBO index regression coefficient values of all EESC and PwLT regression model results. (b) Probability distribution of the SAM index regression coefficient values of all EESC and PwLT regression model results. (c) Probability distribution of the EP flux regression coefficient values of all EESC and PwLT regression model results. Indicated in the figure are also the 0.5 %, 2.5 %, mean, median, 97.5 % and 99.5 % probability values of trends and correlations.

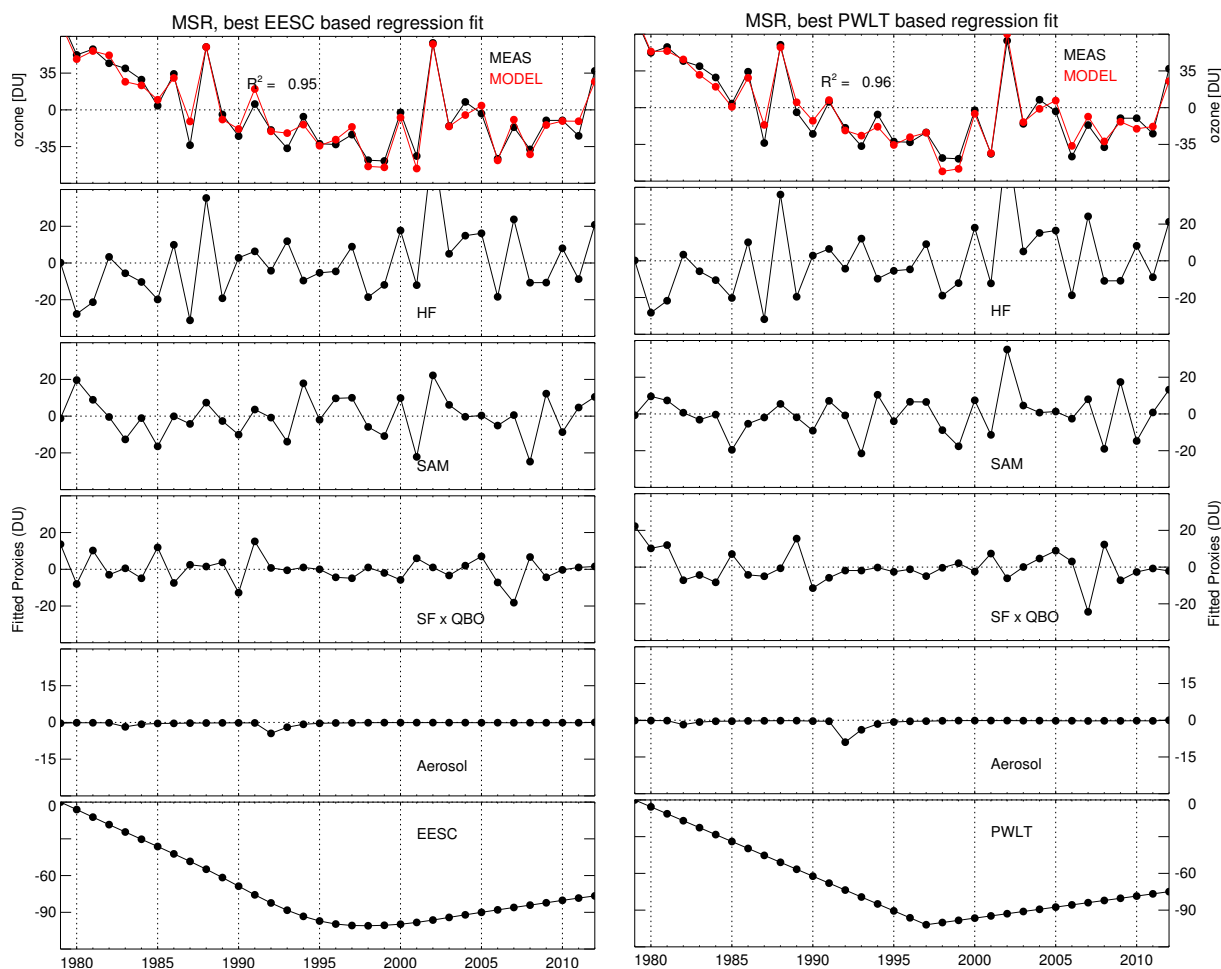


**Figure 8.** Optimal regression model result for the EESC and PWLT and regressions (upper panels, red line) as well as the corresponding ozone record scenario (upper panel, black line). The ozone variations attributable to each are also shown. Ozone and ozone anomalies are given in DU.

canic aerosols and the combined QBO–solar-flux index in the regressions.

We find, consistent with expectations, a robust gradual small increase in Antarctic ozone since the late 1990s that can be attributed to decreases in ODSs for selected combinations of regressors, although the magnitude of the increase is rather uncertain ( $+1.66$  to  $+4.74$  DU year $^{-1}$ ; 95 % CI).

The limited information present in the Antarctic ozone record for volcanic aerosols (essentially two isolated peaks) is consistent with Knibbe et al. (2014), who found little evidence for volcanic effects on total ozone throughout the Southern Hemisphere. Furthermore, Poberaj et al. (2011) also reported little impact of volcanic aerosols from the Pinatubo eruption on Southern Hemispheric ozone, attributing it to dynamical conditions favoring more poleward transport of ozone from the tropics and midlatitudes than usual, thereby “overcompensating [for] the chemical ozone loss ... and reduc[ing] the overall strength of the volcanic ozone signal”.

The lack of correlation between Antarctic ozone and the solar-flux–QBO combined index was also found by Knibbe et al. (2014) for both Antarctic (and Arctic) ozone trends. This lack of QBO–solar signal in Antarctic springtime ozone – also, for example, reported in both Labitzke (2004) and Roscoe and Haigh (2007) – may be related to the dominance in absolute values of the ozone change of ozone depletion and vortex dynamics over potential indirect solar influences on Antarctic springtime ozone.

From our analysis it remains unclear what the appropriate time window would be over which to average the ozone record and the EP flux. Results indicate that the best regression occur for ozone averaged over a time window that includes the ozone hole season – typically September and part of October. On the other hand, the time window should also not extend far beyond the ozone hole season as more and more non-photochemical ozone variations are introduced in the averaged ozone with a longer averaging period. Similarly, for the EP flux we find that including both August

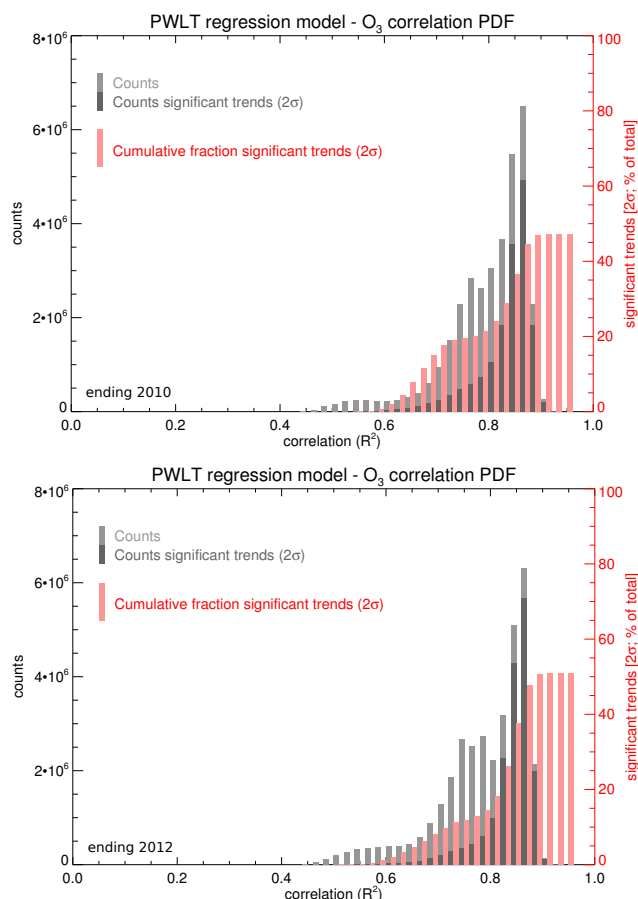


**Figure 9.** The probability distribution of regression-model–ozone-record-scenario correlations ( $R^2$ ) as shown in Fig. 5 for the PWLT regressions and the cumulative fraction of statistically significant ( $2\sigma$ ) ozone trends for each correlation interval (red, right axis). The upper panel shows the distribution for the regressions ending in 2010, and the lower panel for the regressions ending in 2012. See also Table 7.

and September results in the best regressions. However, the choice for using complete calendar months is rather arbitrary, and better choices may exist; this is left for future research.

The lack of a proper definition of appropriate time windows drives our recommendation that care has to be taken with drawing firm conclusions about ozone recovery in the Antarctic ozone hole based on multivariate regression of Antarctic vortex average ozone. It is tempting to discard those results in the full ensemble that do not confirm our expectations, but without proper justification of what constitutes the best set of independent explanatory variables – for example physically compelling arguments – there is the danger of working towards an expected answer.

Another last finding is that a longer post-break period does not necessarily always results in more significant trends, which provides yet another indication to remain careful with drawing too firm conclusions from multivariate regressions.

On the other hand, it can be expected that, by extending the ozone record and using a multivariate regression method to remove well-selected non-ODS influences from the total ozone record, the second stage of ozone recovery in the Antarctic ozone hole will be detectable before the year 2020. Future updates of the analysis in this paper by extension of the present-day ozone records will rather soon provide indications of whether this moment is fast approaching or not.

**The Supplement related to this article is available online at doi:10.5194/acp-15-79-2015-supplement.**

*Acknowledgements.* The authors wish to thank the following authors of chapter 3 of the 2014 WMO ozone assessment report – Sophie Godin Beekmann, Martin Dameris, Peter Braesicke, Martin Chipperfield, Markus Rex and Michelle Santee – as well as John Pyle, Ted Shepherd and, in particular, Paul Newman for encouraging us to write this paper.

Edited by: M. Dameris

## References

- Ammann, G., Meehl, A., Washington, W. M., and Zender, C. S.: A monthly and latitudinally varying volcanic forcing dataset in simulations of 20th century climate, *Geophys. Res. Lett.*, 30, 1657, doi:10.1029/2003GL016875, 2003.
- Andrews, D. G., Holton, J. R., and Leovy, C. B.: *Middle Atmosphere Dynamics*, Academic Press, Orlando, Florida, 489 pp., 1987.
- Anet, J. G., Rozanov, E. V., Muthers, S., Peter, T., Brönnimann, S., Arfeuille, F., Beer, J., Shapiro, A. I., Raible, C. C., Steinhilber, F., Schmutz, W. K.: Impact of a potential 21st century “grand solar minimum” on surface temperatures and stratospheric ozone, *Geophys. Res. Lett.*, 40, 4420–4425, doi:10.1002/grl.50806, 2013.
- Bekki, S., Bodeker, G. E. (Coordinating Lead Authors), Bais, A. F., Butchart, N., Eyring, V., Fahey, D. W., Kinnison, D. E., Lange-matz, U., Mayer, B., Portmann, R. W., Rozanov, E., Braesicke, P., Charlton-Perez, A. J., Chubarova, N. E., Cionni, I., Diaz, S. B., Gillett, N. P., Giorgetta, M. A., Komala, N., Lefèvre, F., McLandress, C., Perlwitz, J., Peter, T., and Shibata, K.: Future ozone and its impact on surface UV, in: *Scientific Assessment of Ozone Depletion: 2010*, Global Ozone Research and Monitoring Project, chap. 3, Report No. 52, 1–516, Geneva, Switzerland, 2011.
- Bunzel, F. and Schmidt, H.: The Brewer–Dobson Circulation in a Changing Climate: impact of the Model Configuration, *J. Atmos. Sci.*, 70, 1437–1455, doi:10.1175/JAS-D-12-0215.1, 2013.
- Crowley, T. J. and Unterman, M. B.: Technical details concerning development of a 1200 yr proxy index for global volcanism, *Earth Syst. Sci. Data*, 5, 187–197, doi:10.5194/essd-5-187-2013, 2013.

- Dameris, M., Matthes, S., Deckert, R., Grewe, V., and Ponater, M.: Solar cycle effect delays onset of ozone recovery, *Geophys. Res. Lett.*, 33, L03806, doi:10.1029/2005GL024741, 2006.
- de Laat, A. T. J. and van Weele, M.: The 2010 Antarctic ozone hole: observed reduction in ozone destruction by minor sudden stratospheric warmings, *Sci. Rep.*, 1, 38, doi:10.1038/srep00038, 2011.
- Dudok de Wit, T., Kretzschmar, M., Lilensten, J., and Woods, T.: Finding the best proxies for the solar UV irradiance, *Geophys. Res. Lett.*, 36, L10107, doi:10.1029/2009GL037825, 2009.
- Ebdon, R. A.: Notes on the wind flow at 50 mb in tropical and subtropical regions in January 1957 and January 1958, *Q. J. Roy. Meteor. Soc.*, 86, 540–542, 1960.
- Engel, A., Möbius, T., Bönisch, H., Schmidt, U., Heinz, R., Levin, I., Atlas, E., Aoki, S., Nakazawa, T., Sugawara, S., Moore, F., Hurst, D., Elkins, J., Schauffler, S., Andrews, A., and Boering, K.: Age of stratospheric air unchanged within uncertainties over the past 30 years, *Nat. Geosci.*, 2, 28–31, doi:10.1038/ngeo388, 2009.
- Eyring, V., Waugh, D. W., Bodeker, G. E., Cordero, E., Akiyoshi, H., Austin, J., Beagley, S. R., Boville, B. A., Braesicke, P., Brühl, C., Butchart, N., Chipperfield, M. P., Dameris, M., Deckert, R., Deushi, M., Frith, S. M., Garcia, R. R., Gettelman, A., Giorgetta, M. A., Kinnison, D. E., Mancini, E., Manzini, E., Marsh, D. R., Matthes, S., Nagashima, T., Newman, P. A., Nielsen, J. E., Pawson, S., Pitari, G., Plummer, D. A., Rozanov, E., Schraner, M., Scinocca, J. F., Semeniuk, K., Shepherd, T. G., Shibata, K., Steil, B., Stolarski, R. S., Tian, W., and Yoshiki, M.: Multimodel projections of stratospheric ozone in the 21st century, *J. Geophys. Res.*, 112, D16303, doi:10.1029/2006JD008332, 2007.
- Fioletov, V. E. and Shepherd, T. G.: Seasonal persistence of mid-latitude total ozone anomalies, *Geophys. Res. Lett.*, 30, 1417, doi:10.1029/2002GL016739, 2003.
- Graystone, P.: Meteorological office discussion on tropical meteorology, *Meteorol. Mag.*, 88, 117, 1959.
- Haigh, J. D.: The impact of solar variability on climate, *Science*, 272, 5264, 981–984, doi:10.1126/science.272.5264.981, 1996.
- Haigh, J. D. and Roscoe, H. K.: Solar influences on polar modes of variability, *Meteorol. Z.*, 15, 371–378, 2006.
- Ho, M., Kiem, A. S., and Verdon-Kidd, D. C.: The Southern Annular Mode: a comparison of indices, *Hydrol. Earth Syst. Sci.*, 16, 967–982, doi:10.5194/hess-16-967-2012, 2012.
- Hood, L.: The solar cycle variation of total ozone: Dynamical forcing on the lower stratosphere, *J. Geophys. Res.*, 102, 1355–1370, 1997.
- Huang, T. Y. W. and Massie, S. T.: Effect of volcanic particles on the O<sub>2</sub> and O<sub>3</sub> photolysis rates and their impact on ozone in the tropical stratosphere, *J. Geophys. Res.*, 102, 1239–1249, doi:10.1029/96JD02967, 1997.
- Jiang, X., Pawson, S., Camp, C. D., Nielsen, J. E., Shia, R.-L., Liao, T., Limpasuvan, V., and Yung, Y. L.: Interannual variability and trends of extratropical ozone. Part II: Southern Hemisphere, *J. Atmos. Sci.*, 65, 3030–3041, doi:10.1175/2008JAS2793.1, 2008.
- Kalnay, E., Kanamitsu, M., Kistler, R., Collins, W., Deaven, D., Gandin, L., Iredell, M., Saha, S., White, G., Woollen, J., Zhu, Y., Leetmaa, A., Reynolds, R., Chelliah, M., Ebisuzaki, W., Higgins, W., Janowiak, J., Mo, K. C., Ropelewski, C., Wang, J., Jenne, R., and Joseph, D.: The NCEP/NCAR 40-Year Reanalysis Project, *Bull. Am. Met. Soc.*, 77, 437–471, 1996.
- Kirtman, B., Power, S. B., Adedoyin, J. A., Boer, G. J., Camilioni, I., Doblas-Reyes, F. J., Fiore, A. M., Kimoto, M., Meehl, G. A., Prather, M., Sarr, A., Schar, C., Sutton, R., van Oldenborgh, G. J., Vecchi, G., and Wang, H. J.: Near-term climate change: projections and predictability, edited by: Stocker, T. F., Qin, D., Plattner, G.-K., Tignor, M. M. B., Allen, S. K., Boschung, J., Nauels, A., Xia, Y., Bex, V. and Midgley, P. M., *Climate change 2013: the physical science basis: contribution to the Fifth Assessment Report of the Intergovernmental Panel on Climate Change*, Cambridge University Press, Cambridge, ISBN 9781107661820, doi:10.1017/CBO9781107415324.023, 2014.
- Klekociuk, A. R., Tully, M. B., Alexander, S. P., Dargaville, R. J., Deschamps, L. L., Fraser, P. J., Gies, H. P., Henderson, S. I., Javorniczky, J., Krummel, P. B., Petelina, S. V., Shanklin, J. D., Siddaway, J. M., and Stone, K. A.: The Antarctic ozone during 2010, *Austr. Meteorol. Oceanogr. J.*, 61, 253–267, 2011.
- Knibbe, J. S., van der A, R. J., and de Laat, A. T. J.: Spatial regression analysis on 32 years total column ozone data, *Atmos. Chem. Phys. Discuss.*, 14, 5323–5373, doi:10.5194/acpd-14-5323-2014, 2014.
- Kramarova, N. A., Nash, E. R., Newman, P. A., Bhartia, P. K., McPeters, R. D., Rault, D. F., Sefstor, C. J., Xu, P. Q., and Labow, G. J.: Measuring the Antarctic ozone hole with the new Ozone Mapping and Profiler Suite (OMPS), *Atmos. Chem. Phys.*, 14, 2353–2361, doi:10.5194/acp-14-2353-2014, 2014.
- Kuttippurath, J., Goutail, F., Pommereau, J.-P., Lefèvre, F., Roscoe, H. K., Pazmiño, A., Feng, W., Chipperfield, M. P., and Godin-Beekmann, S.: Estimation of Antarctic ozone loss from ground-based total column measurements, *Atmos. Chem. Phys.*, 10, 6569–6581, doi:10.5194/acp-10-6569-2010, 2010.
- Kuttippurath, J., Lefèvre, F., Pommereau, J.-P., Roscoe, H. K., Goutail, F., Pazmiño, A., and Shanklin, J. D.: Antarctic ozone loss in 1979–2010: first sign of ozone recovery, *Atmos. Chem. Phys.*, 13, 1625–1635, doi:10.5194/acp-13-1625-2013, 2013.
- Labitzke, K.: On the signal of the 11-Year sunspot cycle in the Stratosphere over the Antarctic and its modulation by the Quasi-Biennial Oscillation (QBO), *Meteorol. Z.*, 13, 263–270, 2004.
- McCormack, J. P. and Hood, L. L.: Apparent solar cycle variations of upper stratospheric ozone and temperature: Latitude and seasonal dependences, *J. Geophys. Res. Atmos.*, 101, 20933–20944, 1996.
- Naujokat, B.: An update of the observed quasi-biennial oscillation of the stratospheric winds over the tropics, *J. Atmos. Sci.*, 43, 1873–1877, 1986.
- Newman, P. A., Nash, E. R., Kawa, S. R., Montzka, S. A., and Schauffler, S. M.: When will the Antarctic ozone hole recover?, *Geophys. Res. Lett.*, 33, L12814, doi:10.1029/2005GL025232, 2006.
- Newman, P. A., Daniel, J. S., Waugh, D. W., and Nash, E. R.: A new formulation of equivalent effective stratospheric chlorine (EESC), *Atmos. Chem. Phys.*, 7, 4537–4552, doi:10.5194/acp-7-4537-2007, 2007.
- Poberaj, C. S., Staehelin, J., and Brunner, D.: Missing stratospheric ozone decrease at Southern Hemisphere middle latitudes after Mt. Pinatubo: a dynamical perspective, *J. Atmos. Sci.*, 68, 1922–1945, doi:10.1175/JAS-D-10-05004.1, 2011.
- Randel, W. J., Wu, F., and Stoarski, R.: Changes in column ozone correlated with the stratospheric EP flux, *J. Meteorol. Soc. Jpn.*, 80, 849–862, 2002.

- Rozanov, E. V., Schlesinger, M. E., Andronova, N. G., Yang, F., Malyshev, S. L., Zubov, V. A., Egorova, T. A., and Li, B.: Climate/chemistry effects of the Pinatubo volcanic eruption simulated by the UIUC stratosphere/troposphere GCM with interactive photochemistry, *J. Geophys. Res.*, 107, 4594, doi:10.1029/2001JD000974, 2002.
- Salby, M. L., Titova, E. A., and Deschamps, L.: Rebound of Antarctic ozone, *Geophys. Res. Lett.*, 38, L09702, doi:10.1029/2011GL047266, 2011.
- Salby, M., Titova, E., and Deschamps, L.: Changes of the Antarctic ozone hole: controlling mechanisms, seasonal predictability, and evolution, *J. Geophys. Res.*, 117, D10111, doi:10.1029/2011JD016285, 2012. Sato et al. (1993), Stratospheric aerosol optical depths, 1850-1990. *J. Geophys. Res.*, 98, 22987–22994, doi:10.1029/93JD02553.
- Solomon, S., Daniel, J. S., Neely, R. R., Vernier, J. P., Dutton, E. G., and Thomason, L. W.: The persistently variable “background” stratospheric aerosol layer and global climate change, *Science*, 333, 6044, 866–870, doi:10.1126/science.1206027, 2011.
- Soukharev, B. E. and Hood, L. L.: Solar cycle variation of stratospheric ozone: multiple regression analysis of long-term satellite data sets and comparisons with models, *J. Geophys. Res.*, 111, D20314, doi:10.1029/2006JD007107, 2006.
- Stiller, G. P., von Clarmann, T., Höpfner, M., Glatthor, N., Grabowski, U., Kellmann, S., Kleinert, A., Linden, A., Milz, M., Reddmann, T., Steck, T., Fischer, H., Funke, B., López-Puertas, M., and Engel, A.: Global distribution of mean age of stratospheric air from MIPAS SF<sub>6</sub> measurements, *Atmos. Chem. Phys.*, 8, 677–695, doi:10.5194/acp-8-677-2008, 2008.
- Telford, P., Braesicke, P., Morgenstern, O., and Pyle, J.: Reassessment of causes of ozone column variability following the eruption of Mount Pinatubo using a nudged CCM, *Atmos. Chem. Phys.*, 9, 4251–4260, doi:10.5194/acp-9-4251-2009, 2009.
- Thompson, D. W. J. and Wallace, J. M.: Annular modes in the extratropical circulation, Part I: Month-to-month variability, *J. Climate*, 13, 1000–1016, 2000.
- United Nations Environment Programme: The Montreal Protocol on Substances that Deplete the Ozone Layer, Nairobi, Kenya, ISBN 978-9966-20-009-9, 2012.
- van der A, R. J., Allaart, M. A. F., and Eskes, H. J.: Multi sensor re-analysis of total ozone, *Atmos. Chem. Phys.*, 10, 11277–11294, doi:10.5194/acp-10-11277-2010, 2010.
- Vernier, J., Thomason, L. W., Pommereau, J., Bourassa, A., Pelon, J., Garnier, A., Hauchecorne, A., Blanot, L., Trepte, C., Degenstein, D., and Vargas, F.: Major influence of tropical volcanic eruptions on the stratospheric aerosol layer during the last decade, *Geophys. Res. Lett.*, 38, L12807, doi:10.1029/2011GL047563, 2011.
- Vyushin, D., Fioletov, V. E., and Shepherd, T. G.: Impact of long-range correlations on trend detection in total ozone, *J. Geophys. Res.*, 112, D14307, doi:10.1029/2006JD008168, 2007.
- Weber, M., Dhomse, S., Wittrock, F., Richter, A., Sinnhuber, B.-M., and Burrows, J. P.: Dynamical control of NH and SH winter/spring total ozone from GOME observations in 1995–2002, *Geophys. Res. Lett.*, 30, 1853, doi:10.1029/2002GL016799, 2003.
- Weber, M., Dikty, S., Burrows, J. P., Garny, H., Dameris, M., Kubin, A., Abalichin, J., and Langematz, U.: The Brewer–Dobson circulation and total ozone from seasonal to decadal time scales, *Atmos. Chem. Phys.*, 11, 11221–11235, doi:10.5194/acp-11-11221-2011, 2011.
- World Meteorological Organization: Scientific Assessment of Ozone Depletion: 2006, Global Ozone Research and Monitoring Project – Report No. 50, Geneva, Switzerland, 572 pp., 2007.
- World Meteorological Organization: Scientific Assessment of Ozone Depletion: 2010, Global Ozone Research and Monitoring Project – Report No. 52, Geneva, Switzerland, 516 pp., 2011.
- Yang, E.-S., Cunnold, D. M., Newchurch, M. J., Salawitch, R. J., McCormick, M. P., Russell III, J. M., Zawodny, J. M., and Oltmans, S. J.: First stage of Antarctic ozone recovery, *J. Geophys. Res.*, 113, D20308, doi:10.1029/2007JD009675, 2008.